SUPPLEMENTAL MATERIAL

METHODS

Chemistry

HPLC. Reverse-phase HPLC (Agilent 1200 Series instrument equipped with UV and radioactivity detectors) was performed using a Zorbax 300SB-C18 column (3.5 μm, 4.6 × 150 mm, Agilent Technologies, Santa Clara, CA) attached to a C18 guard column (Agilent) to determine radiochemical purity. Mobile phase A = 10 mM Et_3N•HOAc, pH 6; and B = CH_3CN was used to apply a linear gradient of 10 – 50% B from 0 – 25 min and 50 – 100% B from 25 – 27 min and detected with radioactivity and A_{220nm} UV-vis absorbance detectors. For stability studies, a gradient of 10 – 50% B from 0 – 20 min; 50 – 100% B from 20 – 25 min; and 100 – 10% B from 25 – 30 min was applied.

Stability Studies. For serum stability studies, 10 μL of 70 μM (1.5 MBq) of [^{64}Cu]L19K-FDNB, [^{64}Cu]L19K-DNP, or [^{64}Cu]L19K was added to 100 μL of a 1:1 solution of fetal bovine serum (FBS):PBS (pH 7.4) and incubated at 37°C for up to 24 h. A 10 μL aliquot was removed after each time point (0, 2, and 24 h) and assayed in the HPLC, detected with the radioactivity detector. For hydrolysis studies with [^{64}Cu]L19K-FDNB, 10 μL of 70 μM [^{64}Cu]L19K-FDNB and 6 μL of 333 μM of unlabeled L19K-FDNB were added to 100 μL of PBS (pH 7.4). The

reaction was incubated at 37°C for up to 24 h and a 10 μL aliquot was removed after each time point (0, 2, and 24 h) for HPLC analysis, detected with radioactivity and at A_{350nm} absorbance.

Biology

Reagents. SDS-PAGE reagents were purchased from Bio-Rad (Hercules, CA). BCA assay kit, silver stain kit, SuperSignal West Pico chemiluminescent substrate, and protease inhibitor formulated with EDTA were purchased from Pierce Thermo-Fisher (Rockford, IL). For flow cytometry, 16B12 monoclonal antibody was purchased from Covance (Berkeley, CA) and FITC-conjugated secondary antibodies were purchased from Abcam (Cambridge, MA). Antibodies used for Western blotting were purchased from Santa Cruz Biotechnology (Santa Cruz, CA). Autoradiography film BX was purchased from Midsci (St. Louis, MO).

Cell Culture. HCT-116 human colorectal cancer cells (ATCC, Manassas, VA) were cultured using Iscove's Modified Dulbecco's Medium formulated with 10% fetal bovine serum (FBS) and 10 μg/mL Gentamicin sulfate (complete media) in a 37ºC humidified chamber containing 5% CO_2. Somatostatin receptor 2-transfected ovarian cancer cells (SSTR2-SKOV3) was cultured using the same

medium with additional 50 μg/mL of Geneticin® (G418) sulfate as a selection antibiotic.

Binding Assays. 10 μL of 5 μM of human VEGF was diluted in 35 μL of PBS (pH 7.4). 5 μL of 5 μM of [^{64}Cu]L19K-FDNB, [^{64}Cu]L19K-DNP, or [^{64}Cu]L19K was added to the VEGF solution with final concentration of 0.5 μM ^{64}Cu-labeled peptide (277 Bq) and 1 μM VEGF. These reactions were incubated at 37°C, overnight. Another reaction comparing the reactivity of [^{64}Cu]L19K-FDNB to human and mouse VEGF homologs was performed following previous methods (*1*), with a final concentration of 1 μM [^{64}Cu]L19K-FDNB (555 Bq) and 0.5 μM of each VEGF homolog. Samples were analyzed via SDS-PAGE, denaturing proteins by heating at 60°C for 5 min and electrophoresed under nonreducing and reducing conditions using a 4 – 20% tris-glycine gel (Bio-Rad, Hercules, CA). The gel was imaged for 5 min using InstantImager™ electronic autoradiography (Packard, Downers Grove, IL) and stained for total protein loading using a silver stain kit (Pierce Thermo-Fisher, Rockford, IL) following supplier's instructions.

For cell binding studies, HCT-116 cells (250 μL of 1×10^6 cells/mL) were adhered in a 24-well plate. The media was replaced with 200 μL of fresh complete media before assay. For in vitro blocking studies, cells were pre-treated with 50 μM of Bevacizumab (Genentech, San Francisco, CA) or 83 μM of unlabeled L19K-FDNB at 4ºC for 1 h. [^{64}Cu]L19K-FDNB was added to a final

concentration of 0.1 μM (277 Bq) and incubated at 4ºC for an additional 1.5 h in the presence or absence of competitor. Cells were pelleted at 4,000 rpm for 3 min, and washed 3× with ice cold PBS. Cell-bound radioactivity was assayed in a Beckman 8000 gamma counter (Beckman Coulter Inc, Brea, CA).

Flow Cytometry. SSTR2-SKOV3 and HCT-116 cells were dissociated from flasks using TrypLE Express cell dissociation reagent. The cells (2 x 10^5) were incubated with 2 μg/mL of HA.11 Clone 16B12 Monoclonal Antibody, targeted to the hemagglutinin epitope on the N-terminus of SSTR2, in PBS containing 2% w/v BSA (PBS-BSA) at room temperature for 30 min. The cells were pelleted and washed with 2 ml of cold PBS, 3×. FITC-conjugated secondary antibody (500 ng/mL) in PBS-BSA was incubated for 30 min at ambient temperature. The cells were pelleted and washed. Controls include no primary antibody or using an IgG control antibody. For analysis and detection of FITC fluorescence, the cells were resuspended in 300 μL of DMEM containing 5% FBS, and 30,000 events per sample were collected and analyzed on a BD FACSAria (Becton Dickinson, San Jose, CA).

Cell Lysis and Western Blot. HCT-116 and SSTR2-SKOV3 cells were lysed using lysis buffer consisting of 50mM Tris (pH 7.5), 150 mM NaCl, 0.5% NP-40, 0.5% sodium deoxycholate, 1% SDS, and 1× protease inhibitor cocktail

formulated with EDTA. Cells (1×10^6) were re-suspended in 500 µL of lysis buffer and sonicated at 10 s bursts, 3×. Cell lysates were heated at 95ºC for 10 min and centrifuged at 14,000 × g for 5 min. Total protein was quantified using BCA assay kit and 10 µg of proteins from each lysate were analyzed by SDS-PAGE under reducing conditions and electroblotted onto a PVDF membrane. The blot was blocked with 3 % bovine serum albumin in PBS for 1 h. For anti-VEGF immunoblotting, 0.5 µg/mL of rabbit anti-hVEGF in tris-buffered saline containing 0.05% tween-20 (TBST) was incubated at 4ºC, overnight. The blot was washed with TBST for 5 min, 3×. Goat anti-rabbit-HRP was incubated for 1 h at ambient temperature and washed with TBST, 5×. For β-actin immunoblotting, anti-β-actin-HRP (50 ng/mL) was incubated for 1 h at ambient temperature. SuperSignal West Pico chemiluminescent substrate was incubated and exposed to classic blue autoradiography film BX.

Small Animal PET/CT Imaging and Biodistribution. Static PET/CT scans were performed using an Inveon MicroPET/CT scanner (Siemens, Knoxville, TN) for 20 min. The images were reconstructed using Maximum A Posteriori Probability (MAP) algorithm and co-registered with CT using image display software (Inveon Research Workplace Workstation, Siemens, Schenectady, NY). Regions of interest (ROI) were drawn for tumor uptake and analyzed as standard uptake values (SUV) using the formula SUV = (MBq/mL) × (animal weight

(g))/injected dose (MBq). For biodistribution studies, mice were sacrificed at indicated time points. Organs and tumors were harvested and weighed. The radioactivity associated with each organ was assayed in a gamma counter, and corrected for background and decay, to determine the percentage of injected dose per gram of organ (%ID/g).

Data Analysis and Statistics. All data were expressed as mean ± SD unless stated otherwise. Statistical analysis was performed using Graphpad Prism version 5 (Graphpad software, San Diego, CA). *P* values were calculated using the Student's t-test when comparing only two groups. One-way ANOVA was used to compare more than two groups with one variable and two-way ANOVA to compare two groups with two variables (ie. peptide and time). Bonferroni restrictions were applied. *P* values with 95% confidence interval ($P < 0.05$) were considered significant.

RESULTS

Mass Spectrometry

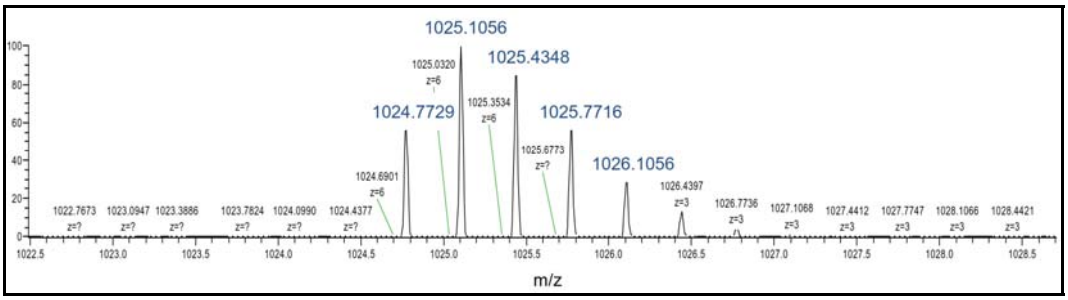

SUPPLEMENTAL FIGURE 1. ESI-MS of L19K-FDNB. The molecular weight was calculated as 3075.2960 from the molecular formula C130 H188 F N36 O44 S3. Theoretical m/z from the triply charged species, $[M+3H]^{+3}$, was calculated as 1025.10, and observed 1025.1056.

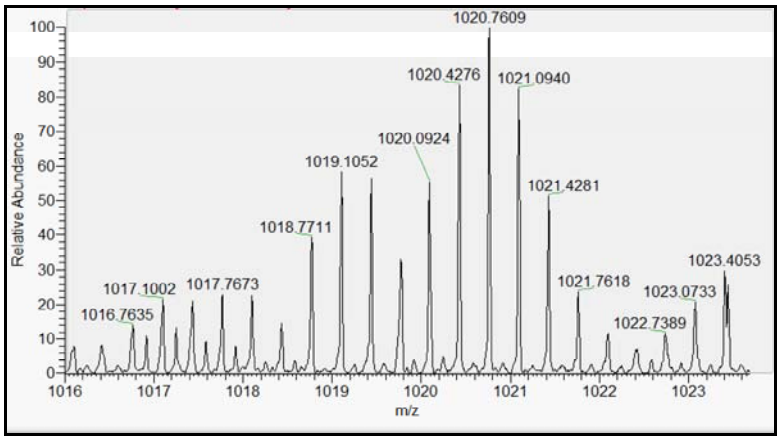

SUPPLEMENTAL FIGURE 2. ESI-MS of L19K-DNP. The molecular weight was calculated as 3054.28 from the molecular formula C130 H189 N36 O44 S3. Theoretical m/z from the triply charged species, $[M+3H]^{+3}$, was calculated as 1019.10, and observed 1020.7609.

Determination of Radiochemical Yield

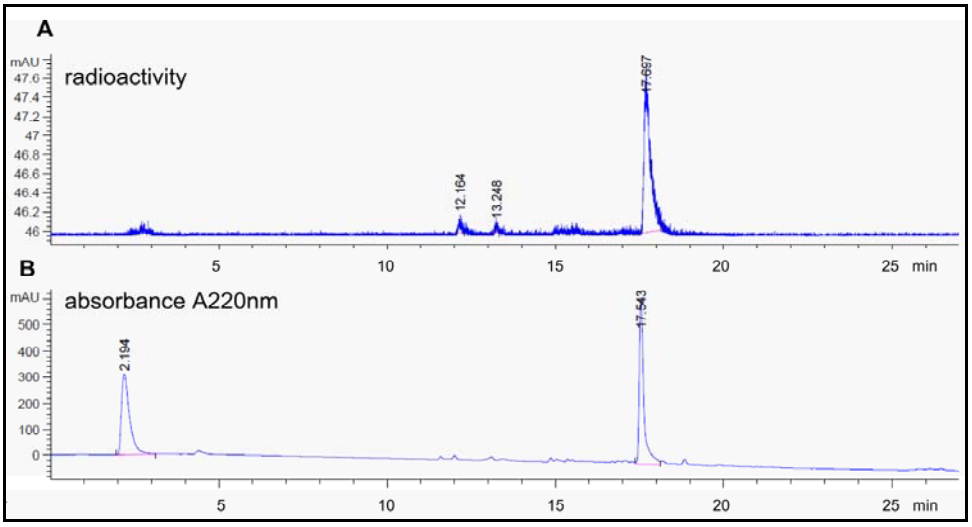

SUPPLEMENTAL FIGURE 3. HPLC chromatograms of [^{64}Cu]L19K-FDNB. The radioactivity trace shows 95% radiochemical yield with retention time at 17.7 min (A) and UV-vis absorbance at A_{220nm} shows the corresponding peptide peak at 17.5 min. The peak at 2.2 min corresponds to the conjugation buffer (B).

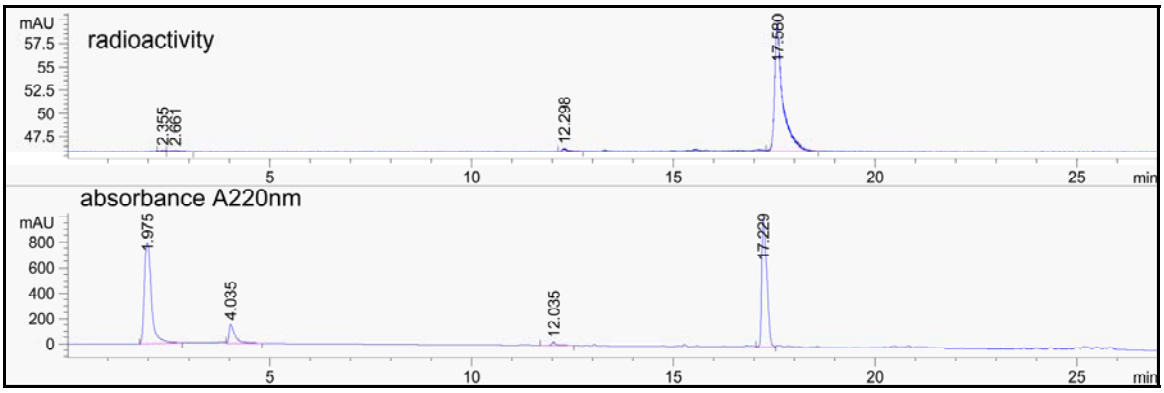

SUPPLEMENTAL FIGURE 4. HPLC chromatograms of [^{64}Cu]L19K-DNP. The radioactivity trace shows 100% radiochemical yield with retention time at 17.6 min (A) and UV-vis absorbance at A_{220nm} shows the corresponding peptide peak at 17.2 min (B).

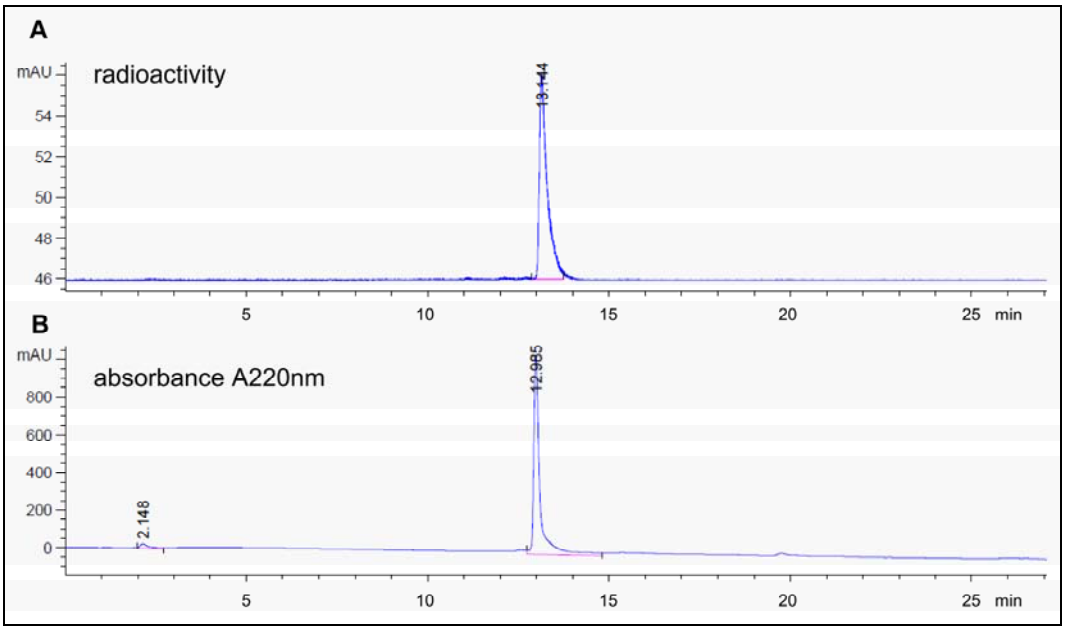

SUPPLEMENTAL FIGURE 5. HPLC chromatograms of [^{64}Cu]L19K. The radioactivity trace shows 100% radiochemical yield with retention time at 13.1 min (A) and UV-vis absorbance at A_{220nm} shows the corresponding peptide peak at 13 min (B).

Stability Studies

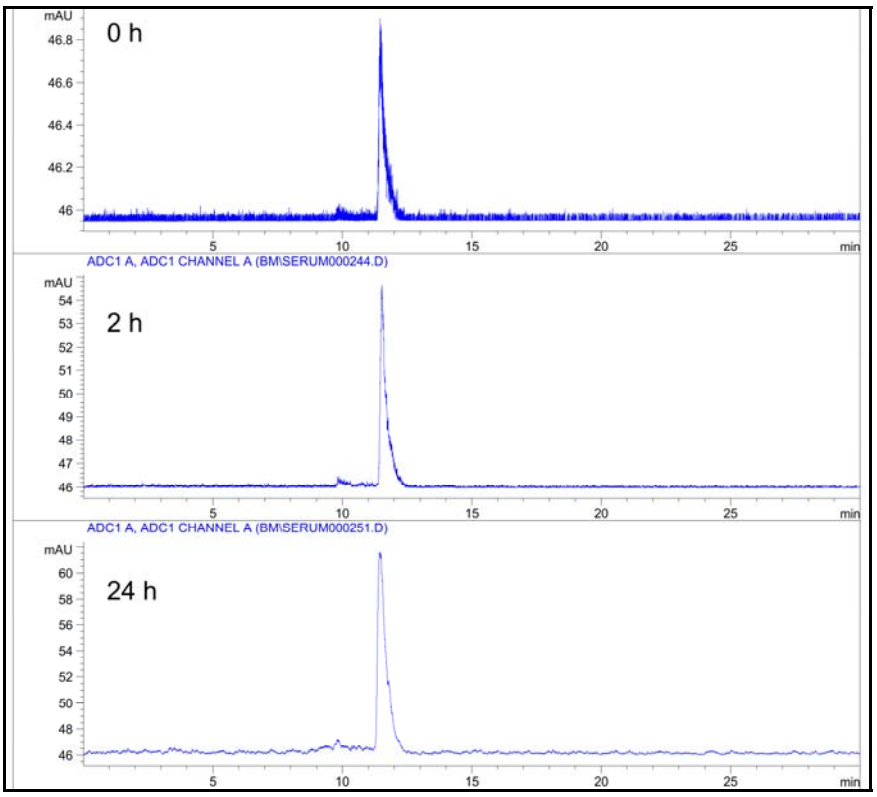

SUPPLEMENTAL FIGURE 6. Serum stability study of [^{64}Cu]L19K. Intact peptide is shown at retention time of 12 min. ^{64}Cu decomplexation was not observed up to 72 h. Some peptide degradation was observed at 10 min but relatively minimal.

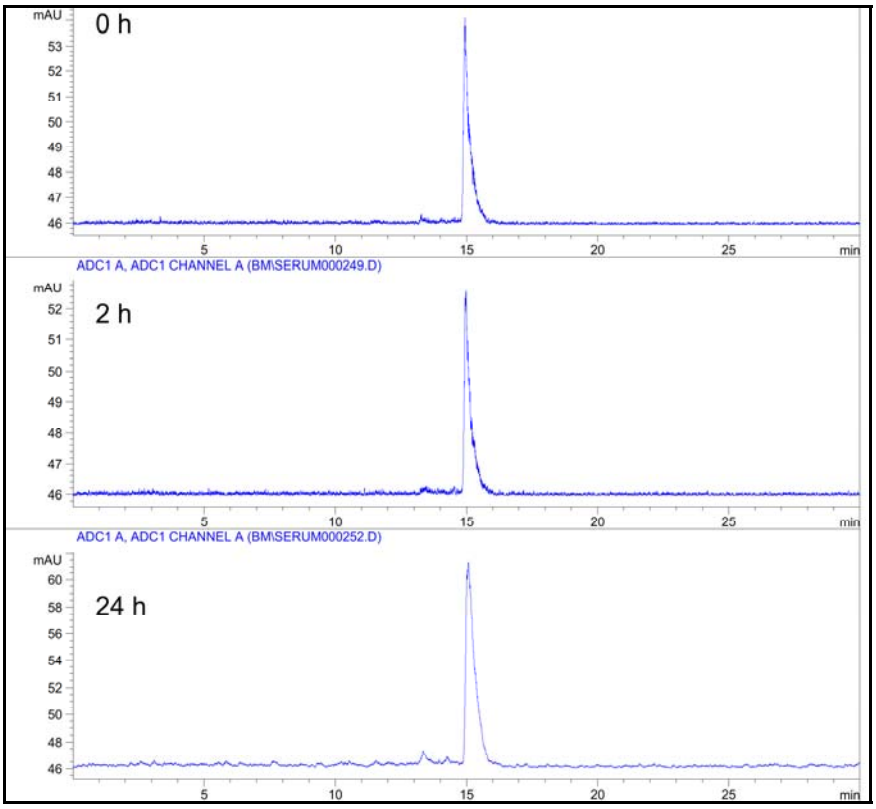

SUPPLEMENTAL FIGURE 7. Serum stability study of [^{64}Cu]L19K-DNP. Intact peptide detected by radioactivity is shown at retention time of 15 min. ^{64}Cu decomplexation was not observed up to 24 h.

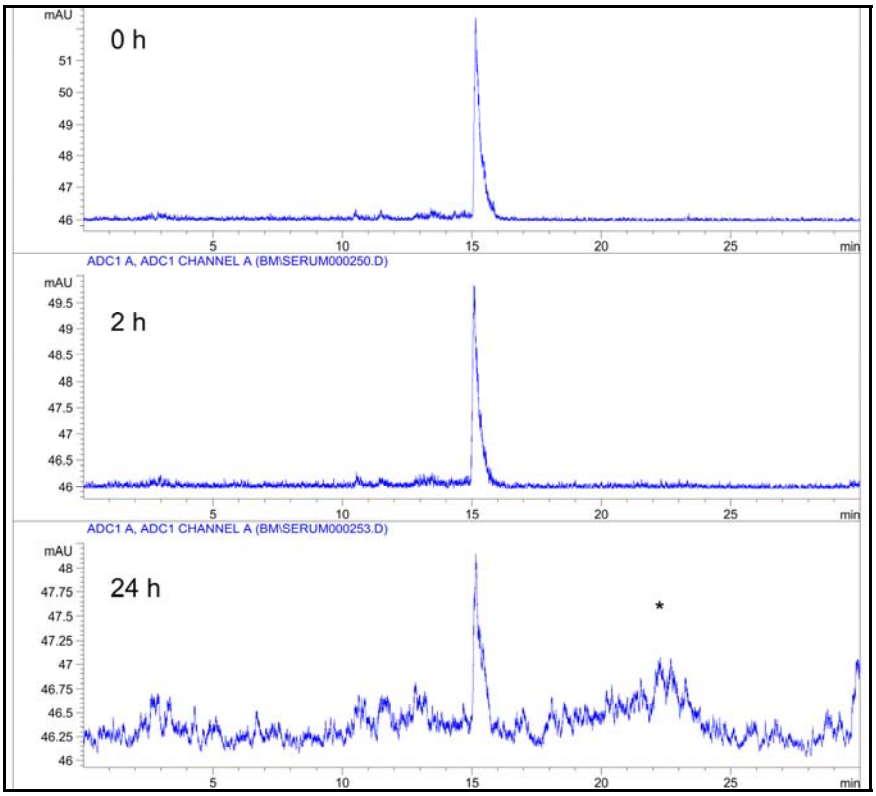

SUPPLEMENTAL FIGURE 8. Serum stability study of [^{64}Cu]L19K-FDNB. Intact peptide detected by radioactivity is shown at retention time of 15.5 min. Initial radiochemical yield of 95% was observed, with free ^{64}Cu at retention time of 2.5 min. ^{64}Cu decomplexation was not observed, however, some cross-reactivity with serum proteins occurred from at 24 h in the absence of VEGF (*).

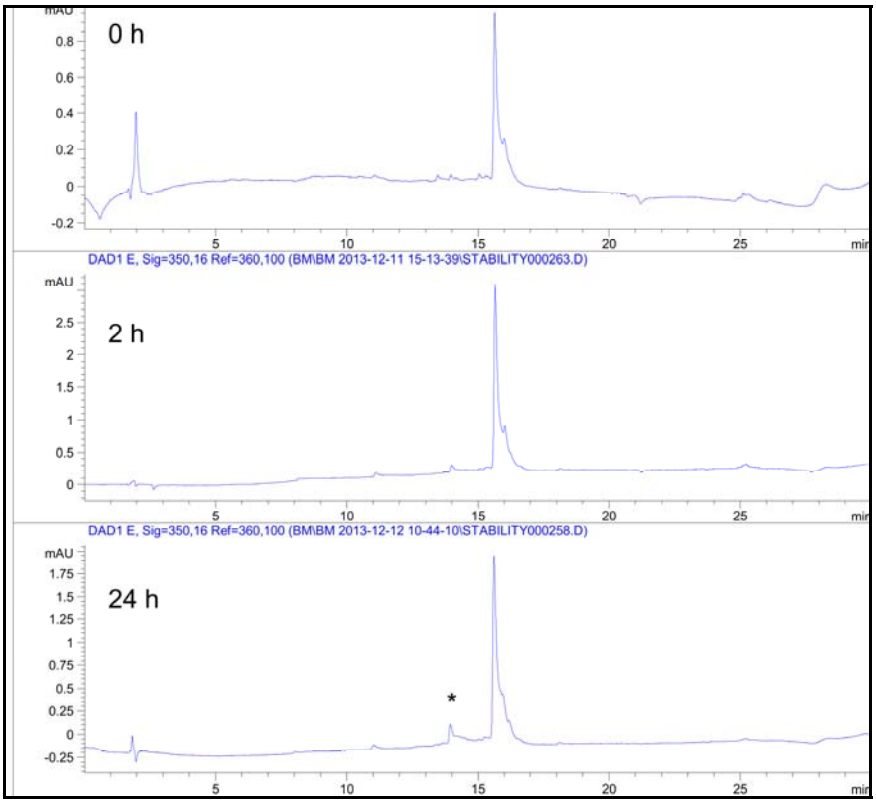

SUPPLEMENTAL FIGURE 9. Stability of L19K-FDNB in PBS. The fluoroaromatic cross-linker moiety of L19K-FDNB is stable in PBS (pH 7.4) with retention time at 15.1 min, detected by A_{350nm} absorbance. The hydrolyzed product is shown at 14 min (*).

[^{64}Cu]L19K-FDNB binding study to human and mouse VEGF in vitro

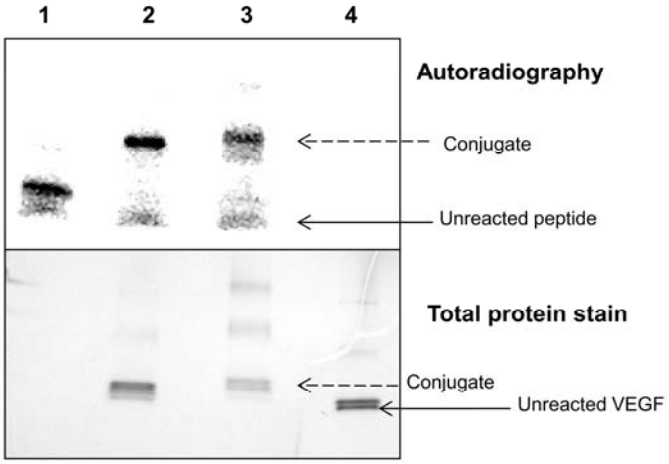

SUPPLEMENTAL FIGURE 10. Autoradiographic SDS-PAGE of [^{64}Cu]L19K-FDNB reactions with human (lane 2) or mouse VEGF (lane 3). Control reactions include [^{64}Cu]L19K-FDNB only (lane 1) and VEGF only (lane 4). Following incubation at 37°C, overnight, each sample was electrophoresed under reducing conditions. The gel was imaged by autoradiography (top panel) and stained for total proteins (bottom panel). Dashed arrows indicate [^{64}Cu]L19K-FDNB-VEGF covalent products, with complete reaction of both VEGF homologs to the peptide.

Characterization of Cells

The expression of somatostatin receptor 2 (SSTR2) has been shown to down-regulate VEGF expression (*2*) thus a transfected cell line, SSTR2-SKOV3, was implanted subcutaneously in mice and used as a low-level VEGF model. HCT-116 xenografts were used as a high-level VEGF model (*3*,*4*). Flow cytometry was

used to determine the integrity of the SSTR2-transfection in SSTR2-SKOV3 cells and western blotting was used to determine VEGF expression. These assays determine positive expression of transfected SSTR2 in SSTR2-SKOV3 cells and higher VEGF expression in HCT-116 cells (Supplemental Figs. 11 – 12).

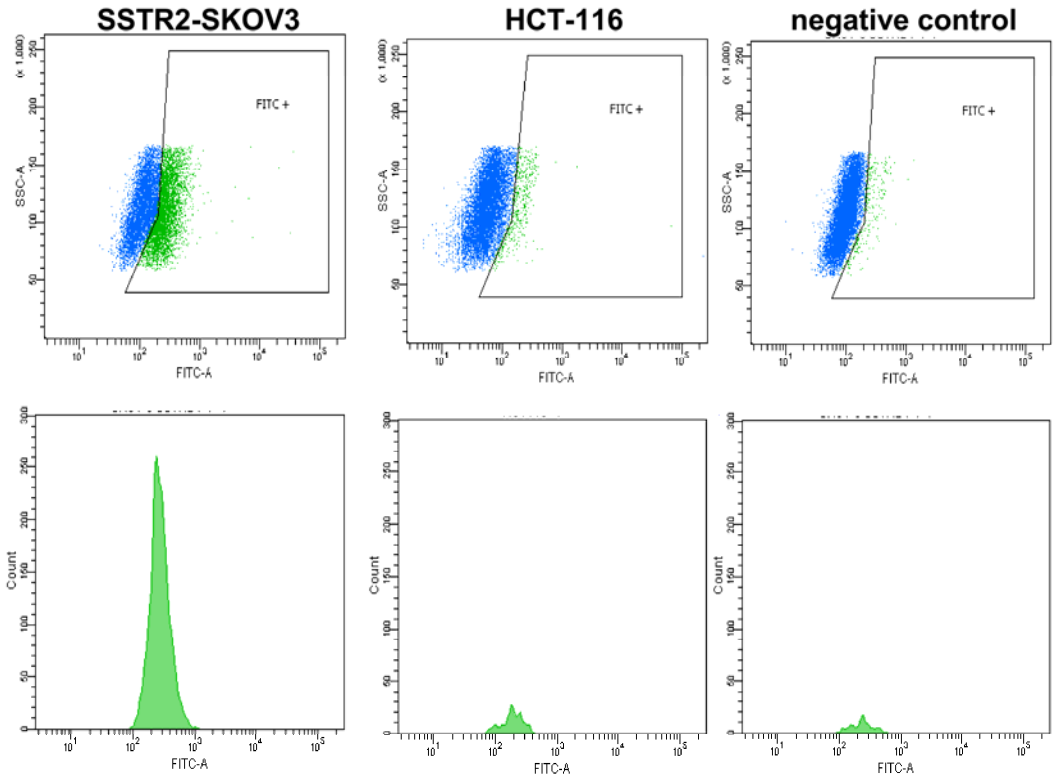

SUPPLEMENTAL FIGURE 11. Flow cytometry histograms of SSTR2-SKOV3 and HCT-116 cells. Both cell lines were stained for the N-terminal tag of SSTR2 to validate transfection integrity in SSTR2-SKOV3 cells. Positive expression was verified in SSTR2-SKOV3 (left panel) shown by the population of cells that emit

fluorescence (green) from the staining assay's secondary antibody, while a negative expression was confirmed in the natural HCT-116 cells with no fluorescence (middle panel). A sample negative control where the primary antibody was omitted in each cell line is shown in the right panel.

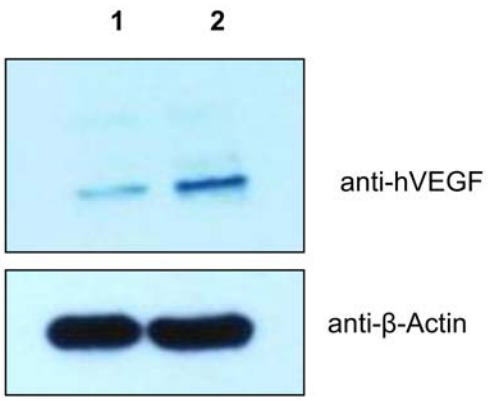

SUPPLEMENTAL FIGURE 12. Western blotting of cell lysates, SSTR2-SKOV3 (lane 1) and HCT-116 (lane 2) confirms a higher level of VEGF expression in HCT-116, using an anti-VEGF immunoassay. Equal protein loading was confirmed using a β-actin immunoassay.

Biodistribution studies of [^{64}Cu]L19K-FDNB in HCT-116 and SSTR2-SKOV3 xenografts

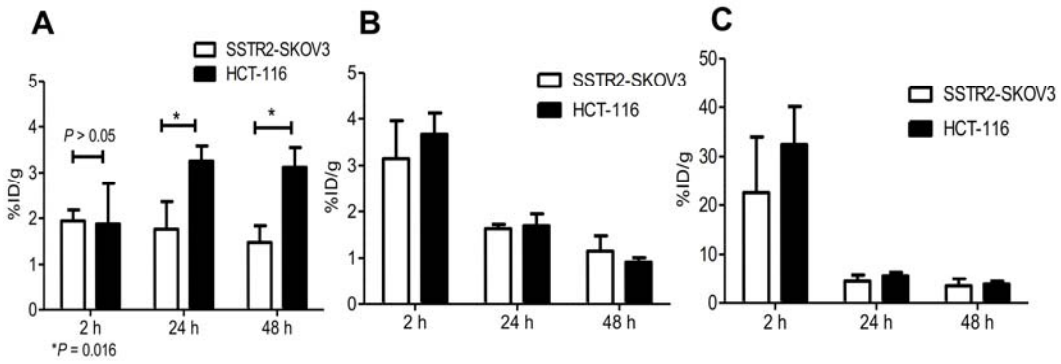

SUPPLEMENTAL FIGURE 13. Biodistribution studies of [^{64}Cu]L19K-FDNB in HCT-116 (high VEGF expressor) and SSTR2-SKOV3 (low VEGF expressor) xenografts highlighting uptake in tumor (A), blood (B), and kidney (C).

SUPPLEMENTAL TABLE 1

Biodistribution of ^{64}Cu-labeled peptides at 24 h p.i. in HCT-116 xenografts

Organ	L19K-FDNB (n = 3)	L19K-DNP (n = 5)	L19K (n = 3)
Blood	1.79 ± 0.17	0.67 ± 0.23	0.37 ± 0.03
Lung	2.25 ± 0.21	1.91 ± 0.40	1.35 ± 0.09
Liver	6.18 ± 1.81	5.05 ± 1.17	4.00 ± 1.20
Spleen	1.38 ± 0.32	0.96 ± 0.16	0.75 ± 0.23
Kidney	4.50 ± 0.89	5.05 ± 1.03	5.77 ± 0.68
Muscle	0.36 ± 0.03	0.26 ± 0.04	0.17 ± 0.03
Fat	0.48 ± 0.09	0.36 ± 0.19	0.15 ± 0.05
Heart	1.42 ± 0.10	1.19 ± 0.18	0.89 ± 0.08
Bone	0.50 ± 0.09	0.39 ± 0.06	0.36 ± 0.02
Tumor	3.94 ± 0.98*	2.43 ± 0.55*	2.83 ± 0.80
Stomach	0.62 ± 0.09	0.77 ± 0.23	0.75 ± 0.34
Sm int	1.29 ± 0.16	1.85 ± 0.38	1.08 ± 0.16
Upper lg int	0.90 ± 0.07	1.73 ± 0.32	0.75 ± 0.13
Lower lg int	1.66 ± 0.30	2.27 ± 0.23	1.61 ± 0.44

Values are %ID/g ± SD. HCT-116 tumor-bearing mice were injected with 7.4 MBq of each ^{64}Cu-labeled peptide via tail vein.
*$P < 0.05$

SUPPLEMENTAL TABLE 2

Biodistribution of ^{64}Cu-labeled peptides at 48 h p.i. in HCT-116 xenografts

Organ	L19K-FDNB (n = 3)			L19K-DNP (n =4)			L19K (n = 3)		
Blood	1.15	±	0.16	0.44	±	0.13	0.48	±	0.19
Lung	2.02	±	0.53	1.52	±	0.19	1.54	±	0.41
Liver	4.13	±	1.21	3.90	±	0.43	3.74	±	1.01
Spleen	0.81	±	0.09	0.71	±	0.15	0.60	±	0.20
Kidney	4.89	±	1.71	4.84	±	1.60	6.57	±	1.72
Muscle	0.34	±	0.03	0.31	±	0.04	0.19	±	0.04
Fat	0.75	±	0.32	0.51	±	0.32	0.62	±	0.07
Heart	1.33	±	0.24	1.19	±	0.28	0.92	±	0.13
Bone	0.46	±	0.15	0.32	±	0.10	0.39	±	0.11
Tumor	2.92	±	0.45	2.28	±	0.41	2.31	±	0.48
Stomach	1.12	±	0.31	0.99	±	0.56	0.90	±	0.26
Sm int	1.76	±	0.40	1.67	±	0.37	1.43	±	0.30
Upper lg int	1.66	±	0.47	1.27	±	0.43	1.37	±	0.20
Lower lg int	1.98	±	0.60	1.46	±	0.28	1.82	±	0.59

Values are %ID/g ± SD.

SUPPLEMENTAL TABLE 3

Biodistribution of ^{64}Cu-labeled peptides at 72 h p.i. in HCT-116 xenografts

Organ	L19K-FDNB (n = 3)	L19K-DNP (n = 3)	L19K (n = 3)
Blood	0.75 ± 0.09	0.43 ± 0.05	0.41 ± 0.04
Lung	1.53 ± 0.25	1.18 ± 0.17	1.18 ± 0.25
Liver	2.96 ± 0.24	2.74 ± 0.28	2.91 ± 0.58
Spleen	0.69 ± 0.05	0.60 ± 0.08	0.55 ± 0.19
Kidney	3.80 ± 0.42	3.31 ± 0.71	5.17 ± 1.25
Muscle	0.28 ± 0.04	0.23 ± 0.01	0.19 ± 0.03
Fat	0.47 ± 0.17	0.45 ± 0.16	0.61 ± 0.27
Heart	1.28 ± 0.16	1.22 ± 0.12	0.98 ± 0.22
Bone	0.32 ± 0.09	0.21 ± 0.07	0.25 ± 0.04
Tumor	2.43 ± 0.23	2.01 ± 0.17	1.90 ± 0.28
Stomach	0.36 ± 0.07	0.45 ± 0.04	0.48 ± 0.13
Sm int	0.99 ± 0.11	0.84 ± 0.13	0.80 ± 0.16
Upper lg int	0.74 ± 0.13	0.82 ± 0.11	0.61 ± 0.12
Lower lg int	1.33 ± 0.21	1.11 ± 0.24	1.15 ± 0.14

Values are %ID/g ± SD.

References

1. Marquez BV, Beck HE, Aweda TA, et al. Enhancing peptide ligand binding to vascular endothelial growth factor by covalent bond formation. *Bioconj Chem.* 2012;23(5):1080-1089.

2. Mei S, Cammalleri M, Azara D, Casini G, Bagnoli P, Dal Monte M. Mechanisms underlying somatostatin receptor 2 down-regulation of vascular endothelial growth factor expression in response to hypoxia in mouse retinal explants. *The Journal of Pathology.* 2012;226(3):519-533.

3. Yin Y, Cao LY, Wu WQ, Li H, Jiang Y, Zhang HF. Blocking effects of siRNA on VEGF expression in human colorectal cancer cells. *World J Gastroenterol.* 2010;16(9):1086-1092.

4. Samuel S, Fan F, Dang LH, Xia L, Gaur P, Ellis LM. Intracrine vascular endothelial growth factor signaling in survival and chemoresistance of human colorectal cancer cells. *Oncogene.* 2011;30(10):1205-1212.